Estimation of Kappa (κ) for a Sedimentary Basin in Greece (EUROSEISTEST) - Correlation to Site Characterisation Parameters

O.-J. Ktenidou, F. Cotton, E. Chaljub
Université Joseph-Fourier, CNRS, Institute of Earth Sciences (ISTERRE), Grenoble, France

S. Drouet
GEOTER International, Roquevaire, France

N. Theodoulidis
Earthquake Planning and Protection Organization – ITSAK, Thessaloniki, Greece

S. Arnaouti
Aristotle University Thessaloniki, Greece

SUMMARY:
Knowledge of the acceleration spectral shape is important for ground motion prediction. At high frequencies spectral amplitude decreases rapidly, controlling peak values. Anderson and Hough (1984) modelled this with the spectral decay factor κ, which constitutes today a basic input parameter –a site effect proxy– for the generation of stochastic ground motion and the calibration and adjustment of GMPEs. We study κ in the EUROSEISTEST valley: a geologically complex and seismically active region with a permanent strong motion array. We derive κ at 14 locations in and around the basin following two approaches: measuring it directly on S-wave spectra and indirectly on the site functions derived from source-path-site inversions. The agreement is good. Because κ is a site-effect proxy, we correlate it with local site conditions: the well-known site-characterisation parameter Vs_{30}, but also the resonant frequency and depth-to-bedrock. We find that these new parameters may complement the existing κ-Vs_{30} correlation.

Keywords: kappa, high-frequency attenuation, site effects, accelerometric arrays, Vs_{30}

1. INTRODUCTION

1.1. Background

Knowing the shape of the acceleration spectrum is important for the prediction of ground motion. At high frequencies, the spectral amplitude decays rapidly, with high frequencies acting as filters on acceleration values. Hanks (1982) first attempted to model this decay through f_{max}, a frequency above which the spectrum 'crashed'. Anderson and Hough (1984) introduced a factor they named the spectral decay factor (κ), which –although empirical rather than theoretical– is used in various applications almost thirty years later. This parameter is based on the observation (Figure 1) that, for frequencies higher than f_e, κ can be related to the slope λ of the spectrum when plotted in lin-ln space:

$$\kappa = -\lambda/\pi \quad \text{where} \quad \lambda = \Delta(\ln a)/\Delta f \tag{1.1}$$

The same authors observed a correlation between observed values of κ and the distance of the source from the station where the record was obtained. As a first approximation they suggested a linear relation where the intercept of the κ trend with distance (denoted κ_0) corresponds to the attenuation that S waves encounter when travelling through the subsurface geological structure to the surface, while the slope of the trend corresponds to the incremental attenuation due to predominantly horizontal S-wave propagation through the crust. If the trend is denoted by *m* then the relation can be written as follows, in units of time:

$$\kappa = \kappa_0 + m \cdot R \quad (s) \tag{1.2}$$

In recent years there have been several studies to investigate the dependence of κ on various factors, such as distance and source parameters (e.g. Tsai and Chen, 2000; Parolai and Bindi, 2004; Douglas et al., 2010; Van Houtte et al., 2011). The debate as to the origins of κ and the effort to decipher them is still on. However, up to now, κ_0 has been correlated primarily to local soil conditions. The following paragraph describes such fields of application.

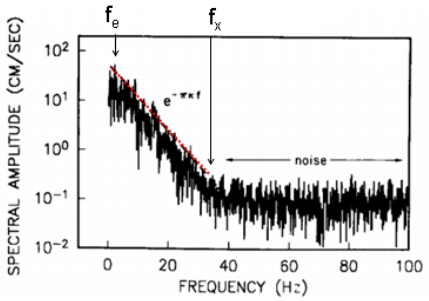

Figure 1. Linear decay trend of the acceleration spectrum when plotted in lin-loge space (adapted from Anderson and Hough, 1984).

1.2. Use of κ in engineering seismology

Despite the on-going debate regarding its origins and though it lacks a rigorous theoretical basis, κ is often used in a variety of applications today, almost 30 years after its definition. It is used in the computation of site amplification factors when using the quarter-wavelength method of Boore and Joyner (1997). It constitutes an important input parameter in the prediction of ground motion and hence in the creation and calibration of GMPEs, particularly for Central and Eastern North America (Toro et al., 1997; Atkinson and Boore, 2006). Also, since these are usually created for hard rock sites, κ is also used when adjusting such models for softer site conditions such as rock. This may be done through the host-to-target method used e.g. by Cotton et al. (2006) and Douglas et al. (2006). κ is also necessary to constrain the attenuation, PGA and duration of synthetic accelerograms generated with stochastic methods in ground motion simulation studies (e.g., Boore, 2003). Finally, κ_0 may be used in site characterisation, especially given empirical correlations of κ_0 with Vs_{30} such as those introduced by Silva et al. (1998). Recently it has been correlated also to other engineering parameters such as the Arias intensity and peak ground acceleration (Mena et al., 2010).

1.3. The present study

Our motivation in this study lies in estimating κ at a site marked by complex surface geology, where site effects have already been studied and have been shown to be of great importance, and where records are available from a variety of geological conditions ranging from soft soil to hard rock. This will allow us to perform two tasks: 1. Estimate κ and particularly κ_0 at all these sites, through two different approaches (directly on the data, based on the original definition; and indirectly, based on a previous site effect study via inversions). 2. Correlate our κ_0 estimates with the local soil conditions, test the validity of κ_0 as a proxy for site effects, and link it to the recent parameters used in site characterisation. In the present work we will assume the simple model of Equation 1.2 for κ, where κ_0 is a site effect and *m* is related to regional (presumably frequency-independent) Q attenuation.

2. STUDY AREA AND DATA

The area studied is an elongated sedimentary basin in Northern Greece, situated between lakes Lagada and Volvi. It lies 30 km from the city of Thessaloniki and is the nearest active seismic zone affecting it. This is why, over the past two decades, this site has been the object of extensive studies in terms of its geological structure and soil properties (through geological, geophysical and geotechnical in situ surveys) and seismic response (through empirical and numerical methods).

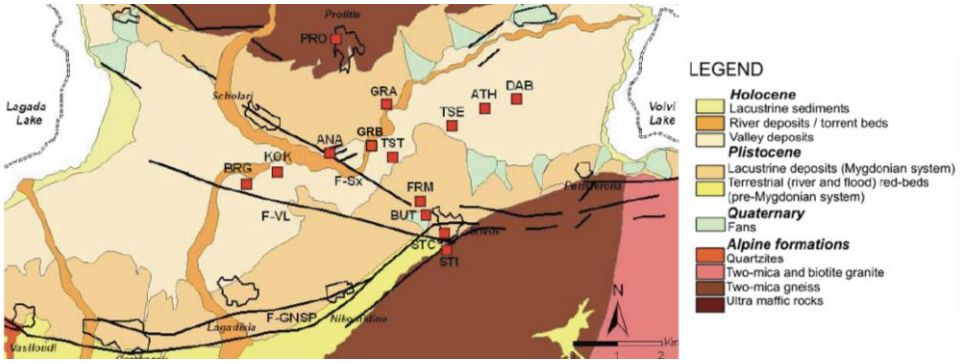

Figure 2. Plan view of the surface stations of the permanent accelerometric network at EUROSEISTEST (adapted from Manakou et al., 2010).

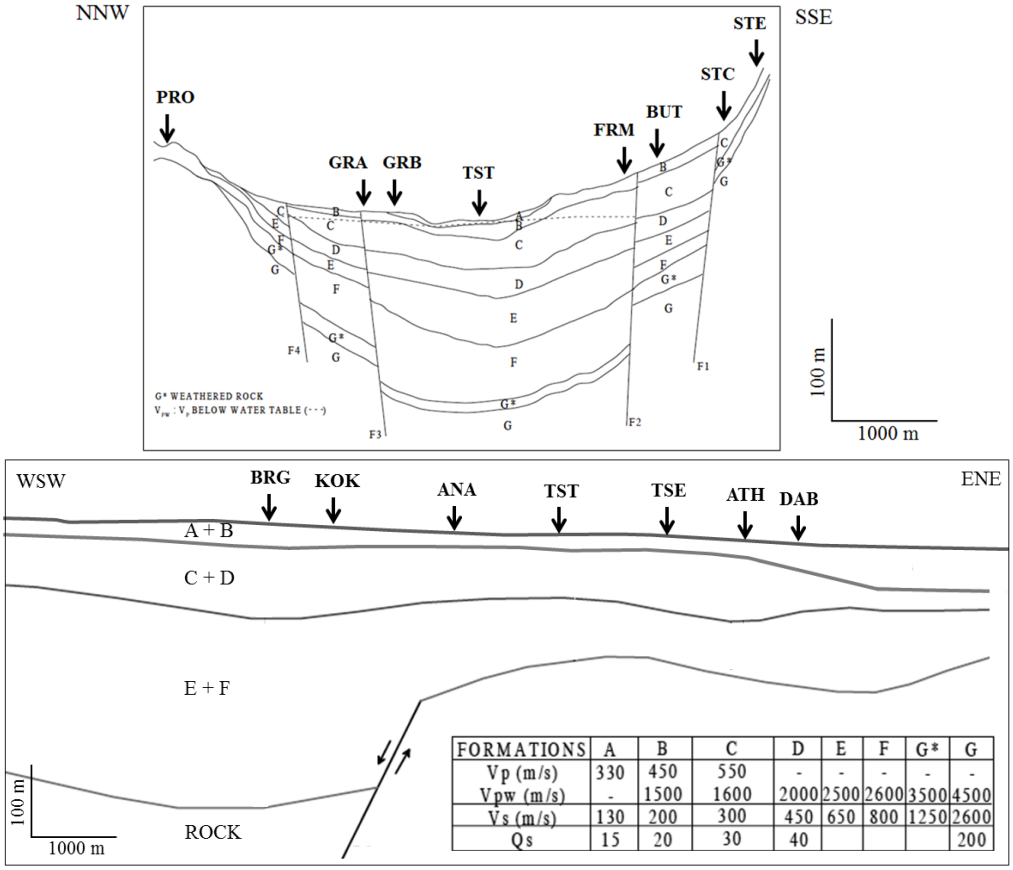

Figure 3. NNW-SSE (adapted from Raptakis et al., 2000 - top) and WSW-ENE cross-sections (adapted from Manakou et al., 2010 - bottom) passing through the centre of the basin. We use arrows to indicate the locations of the stations.

The basin's width is around 6 km and the maximum thickness of the sediments is around 200 m at its centre. A permanent accelerometric network named Euroseistest (http://euroseis.civil.auth.gr) has been installed around the basin centre, comprising 14 surface and 6 downhole receivers. The surface layout of the array has the shape of a cross, extending in two directions, perpendicular and parallel to the basin axis. The stations have been installed in different types of soil and rock formations (Figures 2 to 4) so as to sample ground motion in various geological conditions. Thus, the soil conditions where κ is investigated range from very soft, deep valley deposits (TST station at the valley centre) to very hard rock outcrop (PRO and STE stations on the neighbouring hills). In terms of shear wave velocity, this corresponds to a range of Vs_{30} from 175 to more than 800 m/s. In terms of EC8 site classification (CEN, 2003), this corresponds to sites ranging from D to A respectively.

We use a dataset of 42 earthquakes, each of which was recorded by at least three of the surface stations of the permanent network between 1994 and 2005, giving 184 three-component records in total. The epicentral distribution of these events is shown in Figure 4. Their magnitudes range from 2 to 6.5. Most distances range from 4 to 60 km, with one distant event recorded at 150 km. All events are crustal, with depths up to 13 km. These parameters are shown in Figure 5.

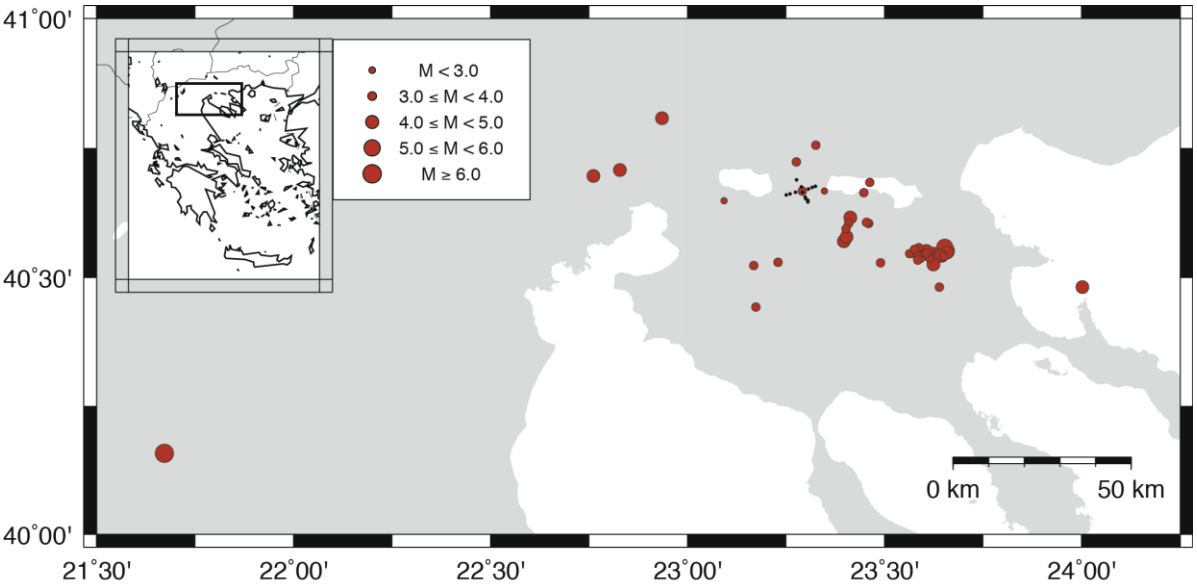

Figure 4. Epicentre distribution for the 42 events of the dataset. The size of the circle scales with magnitude. Location of the array stations is marked. Distances in the legend are in km.

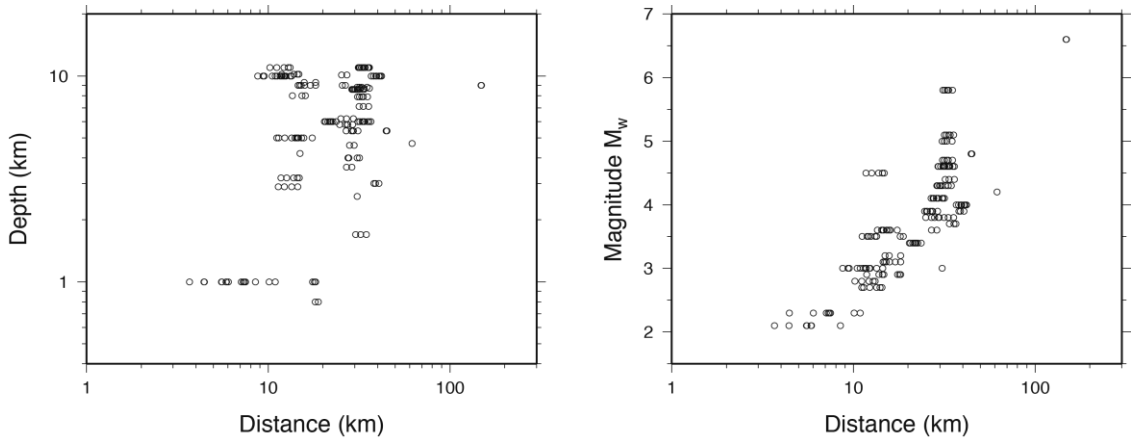

Figure 5. Magnitude and depth distribution of the dataset vs. epicentral distance.

3. APPROACH 1: ACCELERATION SPECTRA

We follow the methodology proposed in Ktenidou et al. (2012) for the estimation of κ. The steps followed are summarised below. We choose records of good quality based on a preliminary visual check, and for which there is an adequate window of pre-event noise recorded. We pick P and S arrivals and choose an S-wave window by visual inspection, taking into account the magnitude and distance of the earthquake. We compute the signal-to-noise ratio using the S-wave and noise windows and only work on data for which SNR is higher than 3. We compute the Fourier amplitude spectrum for the S-window and pick the frequencies f_e and f_x for which the spectral acceleration amplitude decreases linearly in lin-log space. We take care to pick f_e avoiding the corner frequency of the

respective earthquakes (f_e>f_c) and –when possible– the resonant peak of the transfer function and the first few overtones (Parolai and Bindi, 2004). f_x is chosen within the frequency range for which the instruments response can be considered as relatively flat. Using the chosen frequency range, we regress the data based on equation (1.1) to compute the individual value of κ for each event and each station. We do this for all three components. We then compute the average horizontal κ value from the NS and EW components. We discard records for which the difference between the two is larger than 25%. Figure 6 shows the picking of f_e and f_x and the computation of κ for the same earthquake (20/04/2005 07:52 GMT, M 4.6, R=32 km, EW component) recorded on two very different sites: TST, the centre of the basin where Vs_{30}=175 m/s, and PRO, a nearby rock outcrop where Vs_{30}>800 m/s (see station locations in Figure 3). f_x is determined by the noise level, which is naturally lower at PRO. f_e is determined by the resonant frequency: it is lower at TST, where f_o=0.5 Hz and higher at PRO, where f_o~12 Hz. The computed κ values differ greatly, as expected: κ is almost double at TST than at PRO.

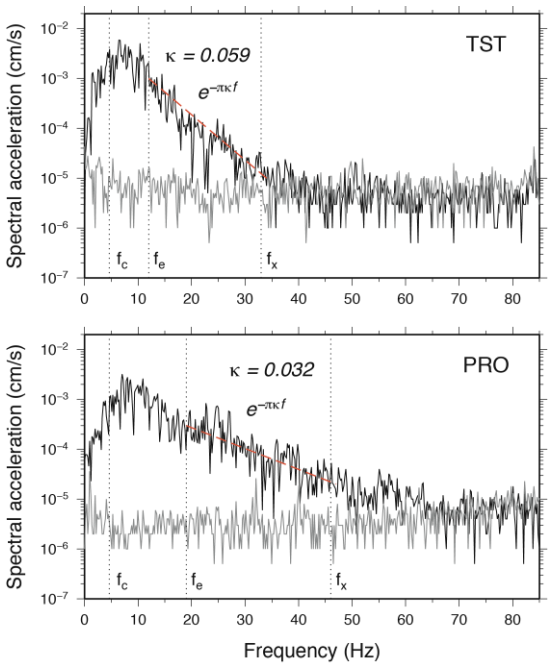

Figure 6. Example of the picking of f_e and f_x and the regression of κ for a simultaneous record at TST (valley centre - top) and PRO (rock outcrop - bottom). Noise spectrum plotted in black, S-window in grey.

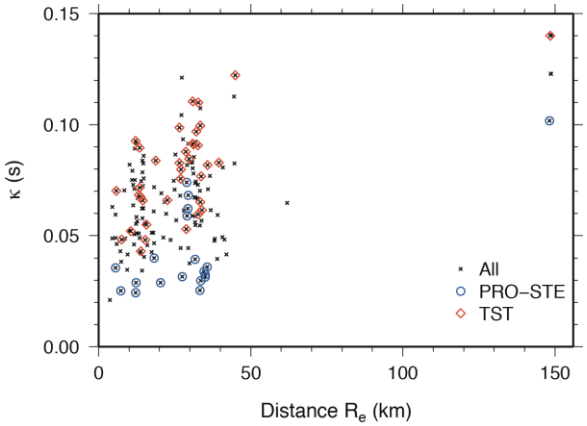

Figure 7. Distribution of individual κ values with distance for the entire dataset (black crosses). We mark results at the softest station in red (TST, valley centre) and at the hardest stations in blue (PRO and STE, rock outcrop).

We now have pairs of values for κ and distance at each site studied. Before proceeding to the regression with distance and derive κ models, we observe the individual values of κ (black crosses in

Figure 7). We see a rather linear trend with distance, even though most of the data come from short distances. At the same time, we find that the scatter, even for those short distances, is quite large. However, despite the scatter, we find that the values of κ are correlated with the site type. In Figure 7 we mark the data points coming from TST site in red and the data points coming from STE and PRO in blue (STE is the other rock site along with PRO). We find the same tendency shown in Figure 6, in that κ is generally larger for the softer site. Most data points coming from intermediate site conditions (i.e., between the centre and the edges of the basin) tend to plot somewhere in between the two.

We can now proceed to the regressions with distance to derive the parameters of equation (1.2), i.e. κ_0 and m. Following the recommendations of Ktenidou et al. (2012) we use a weighed bisquared regression scheme. This robust regression allows us to make use of the very scarce data (only one event) available at 150 km without permitting it to force the slope of the regressed line. Given that the slope of the line is considered to represent the regional attenuation effect, we decide it must be the same for all stations. Thus, we compute the slope using data from all the stations together, regardless of soil type. We can then proceed with the estimation of κ_0 for different site conditions, constraining the slope to the computed value. We choose to compute κ_0 for three different cases:

1. For the entire dataset, using all stations together, in order to get an overall estimate
2. For each station separately
3. Grouping the stations with respect to the local site conditions, namely Vs_{30}, based on the observation in Figure 7. This grouping corresponds to a rough 'soft soil - stiff soil - rock' classification.

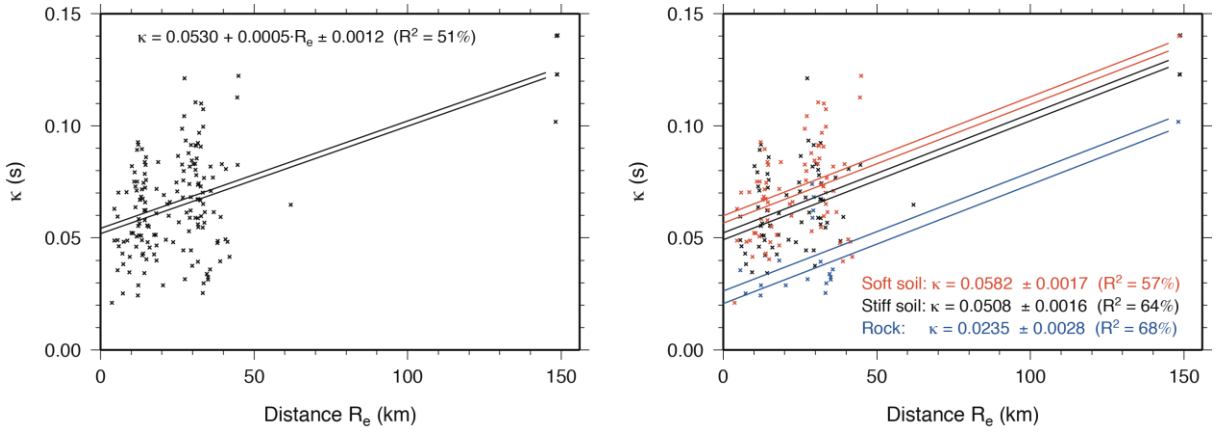

Figure 8. Distribution of individual κ values and regression with distance for cases 1 (entire dataset – left) and 3 (sites grouped based on Vs_{30} – right). Regressed lines plotted ± 1 standard deviation.

The results are shown in Figure 8 for cases 1 and 3. The correlation coefficient is around 50% in case 1 and improves with the grouping in case 2, particularly for the rock site group, where it reaches almost 70%. We note that although there is only one event at distance 150 km, nevertheless the observed κ values at that distance are well correlated to the Vs_{30} values. Thus, the distinction between the groups holds within the entire distance range. In case 1, the relatively high average value of κ_0 (0.053 s) is determined by the majority of stations being located on soil. In case 3, the κ_0 values derived from the site categorisation correlate with the Vs_{30} values, reinforcing the notion that these two parameters are related. However, though the difference in κ_0 is very clear between rock and soil, it is not as striking between the different kinds of soils. We believe this is due to the larger scatter observed in κ values in soil. We will address this issue further using the results of case 2 in Section 5.

4. APPROACH 2: SOURCE-PATH-SITE INVERSIONS

In Section 3 we computed κ according to the original definition introduced by Anderson and Hough (1984). In this section we follow an alternative approach. Drouet et al. (2008b) implemented a

parametric inversion on the same dataset we have studied here and separated the source, path and site contribution to the site response. Their technique is detailed in Drouet et al. (2008a) and is based on far-field Fourier spectra of S waves. A Brune source is assumed and both geometrical and anelastic attenuation are modeled. Then an iterative least squares inversion is applied which uses the derivatives of the modeling function with respect to the different parameters. Drouet et al. (2008b) derived moment magnitudes, corner frequencies, a frequency-dependent model of Q and the site functions for the average horizontal and vertical component. Here we focus on the latter two.

First, we use the high-frequency part of the amplification functions they computed at each station to derive the site-specific component of κ, namely κ_0. This alternative way to compute κ_0 has been applied before by Drouet et al. (2010). The frequency range in which we consider the decay of the transfer functions linear ranges from f_e=5-15 Hz to f_x=15-25 Hz and is shown in Figure 9 along with the computation of κ_0 from the inverted amplification.

In Figure 9 we also compare the κ_0 values computed with the two different approaches: case 2 following the Anderson-Hough method of the previous section, and κ as the decay of the inverted amplification). The results are very similar. This supports the notion that κ_0 is primarily a site effect, since in the second approach source and path effects have been accounted for separately. Overall, κ_0 values from the two approaches range from 0.02 to 0.08 s for these highly varying site conditions, with an average of 0.053 s. Hatzidimitriou et al. (1993) proposed an average κ_0 value of 0.057 s after studying a variety of sites across Greece. Ktenidou et al. (2012) found lower values of 0.02-0.03 s near the Gulf of Corinth.

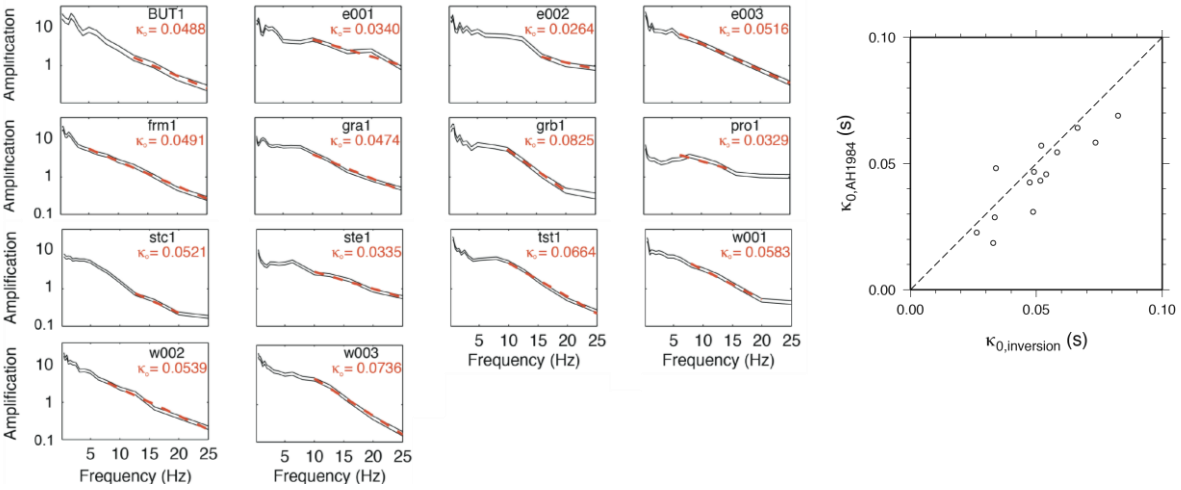

Figure 9. Left: Site functions (average ± 1 standard deviation) for all stations are shown in black. Computation of κ_0 from their high-frequency part is shown in red. Right: Correlation of κ_0 values using the two approaches: the inverted site function and the Anderson and Hough (1984) method.

Finally, it is also possible to compare the values of anelastic Q attenuation derived from the two approaches. Drouet et al. (2008b) find the following relation:

$$Q(f) = 82.68 \times f^{0.60448} \tag{4.1}$$

The frequency range in which their data was analysed was between 5 and 25 Hz. The frequency range we used to compute κ was mostly 10 to 30 Hz. For 20 Hz, an average frequency value of our range, according to (4.1) Q is around 505. Indeed, assuming an average crustal shear wave velocity of 3.5 km/s, the slope we computed in our κ regressions in Figure 8 (m~0.0005 s/km) corresponds to a frequency-independent Q of about 570. So the two approaches yield similar results also in terms of Q and both indicate a highly attenuative region. Similar low Q values are also proposed for Northern Greece by Hatzidimitruou (1995) and for the Corinth Gulf by Ktenidou et al. (2012).

5. CORRELATION WITH SITE CHARACTERISATION PARAMETERS

We make use of the information available from the extensive geological, geophysical and geotechnical surveys already conducted at EUROSEISTEST (Raptakis et al., 2000; Manakou et al., 2010) in order to correlate κ with the main parameters used in site characterization. We use the κ_0 values computed at each station of the array in Sections 3 (case 2) and 4. The main parameter that κ has already been correlated to is Vs_{30}, which is also the main parameter used until recently for site classification. However, the most recent trends in site characterization do not restrict themselves to the upper 30 m, but also include some parameter that indicates the conditions at larger depths (e.g., Luzi et al., 2011; Pitilakis et al., 2011). This is usually achieved through the fundamental frequency (or period) or the depth to bedrock, which may be defined in different ways. Hence, here we choose to investigate the relation not only between κ_0 and Vs_{30} but also with these two newer parameters, f_{res} and $H_{bedrock}$ (by bedrock we mean formations G/G* of Figure 3). In Figure 10 we see indeed a correlation between κ_0 and all three parameters, and the correlation coefficient is of the order of 30%, similar in all cases.

Despite the correlation, it is evident from Figure 10 that for soil sites with Vs_{30} from 180 to 300 m/s there is a large scatter in κ_0 values. This means that sites belonging to the same site class (class C, according to EC8) exhibit very different responses in terms of attenuation, which would render it difficult to propose typical values for the class. We suggest that this may be partly explained by the other two parameters which are linked to the deeper structure: f_{res} and $H_{bedrock}$. In this site, as seen in Figure 3, the underlying structure of the basin causes sharp variations in these two parameters. In Figure 11 we apply a colour code to separate very deep soft sites (red) from shallower soft sites (blue). The deeper sites tend to exhibit higher κ_0 values.

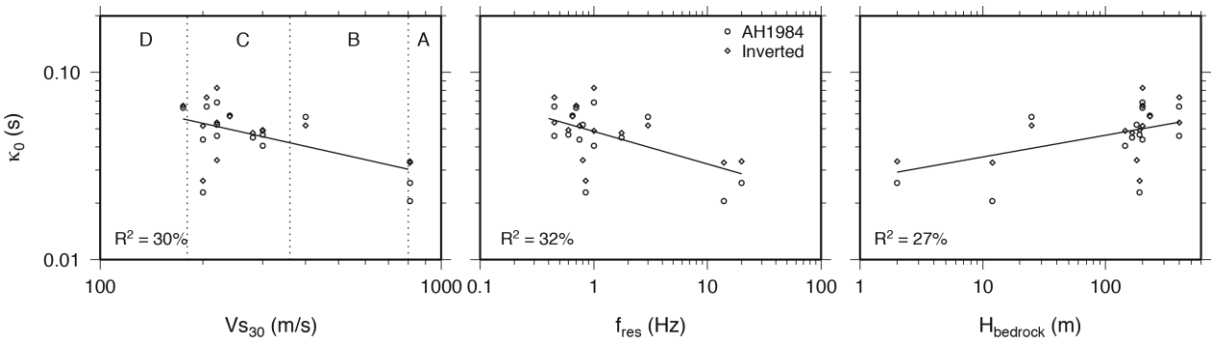

Figure 10. Correlation of κ_0 values from the two approaches (inverted site function and Anderson and Hough, 1984) with site characterization parameters: Vs_{30}, resonant frequency and depth to bedrock. Correlation coefficient is also shown. Vertical lines indicate limits between EC8 site classes A to D.

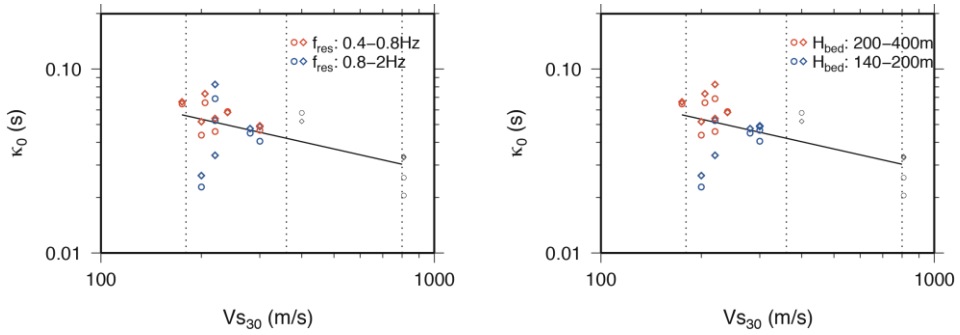

Figure 11. Correlation of κ_0 with Vs_{30}, colour-coded for different ranges of resonant frequency (left) and depth to bedrock (right).

The existing empirical correlations between κ_0 and Vs_{30} have been made mainly in the context of hard rock-to-rock conversions, so the data came mainly from sites where Vs_{30}>400m/s. Such correlations

include those of Silva et al. (1998), Drouet et al. (2010), and Edwards et al. (2011). Van Houtte et al. (2011) proposed correlations for rock sites using different kinds of average Vs as well as the resonant frequency. Though here we have generally softer sites, in Figure 12 we attempt a comparison of our results with the predicted κ_0 values. For stiff soil and rock (site classes A and B), most existing empirical correlations predict κ_0 accurately. If combined and extended out of their range of application into that of soft soil (classes A and B), they provide upper and lower bounds for the κ_0 we computed.

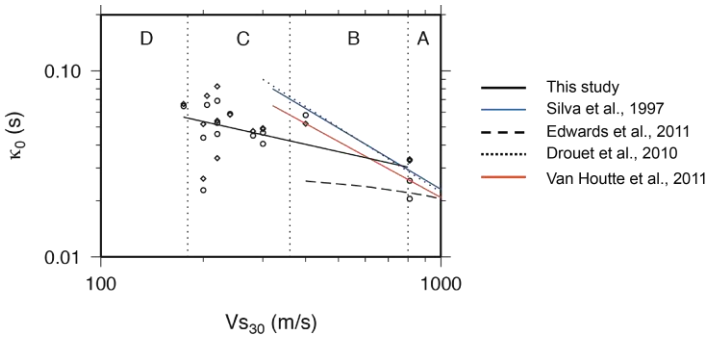

Figure 12. Correlation of κ_0 with Vs_{30} and comparison with predictions from empirical correlations.

6. CONCLUSIONS

We study κ in the EUROSEISTEST valley: a geologically complex and seismically active region with a permanent strong motion array. We use the surface stations of the array to compute κ at 14 locations in and around the basin. We follow two approaches: 1. We measure it directly on S-wave spectra according to the Anderson-Hough (1984) method and then make a regression with distance to derive the site-specific component, κ_0. 2. We compute it indirectly on the site functions derived from source-path-site inversions at each station of the array. The agreement between the two approaches is good in terms of both site-specific κ_0 and regional anelastic Q attenuation. We focus on κ_0 values, which range from 0.02 s to 0.08 s depending on the type of site. As expected, κ_0 increases for soft sites, but so does the scatter. Because κ is a site-effect proxy, we examine its correlation with local site conditions. We choose three parameters: the well-known site-characterisation parameter Vs_{30}, for which empirical correlations already exist, and two parameters that have been used recently to account for surface geology below 30 m: the resonant frequency and the depth to bedrock. We find that κ_0 is correlated (R^2=30%) to all three parameters. We believe that to some extent, the parameters indicating the deeper surface structure may complement the existing κ-Vs_{30} correlations and help interpret some of its scatter. For instance, we find large scatter in κ_0 for class C sites, which is partly explained when we group them according to resonant frequency and bedrock depth.

ACKNOWLEDGEMENTS

The accelerograms used were produced by the EUROSEISTEST array (http://euroseis.civil.auth.gr). The research for κ estimation and the drafting of the paper were funded by European research project SHARE (Seismic Hazard Harmonization in Europe, contract number 226967), while the source-site-path inversions were conducted under Marie Curie Actions-TOK/DEV (MTKD-CT-2005-029627, ITSAK-GR). Signal processing benefited from SAC2008 (http://www.iris.edu/software/sac; Goldstein et al., 2003) and some figures were made using Generic Mapping Tools v. 3.4 (www.soest.hawaii.edu/gmt; Wessel and Smith, 1998).

REFERENCES

Anderson, J.G. and S.E. Hough (1984). A model for the shape of the fourier amplitude spectrum of acceleration at high frequencies, *Bull. Seism. Soc. Am.* **74**, 1969-1993.

Atkinson, G.M. and D.M. Boore (2006). Earthquake Ground-Motion Prediction Equations for Eastern North America, *Bull. Seism. Soc. Am.* **96**, 2181-2205.

Boore, D.M. (2003), Simulation of ground motion using the stochastic method, Pure Appl. Geoph. **160**, 635-676.

Boore D.M. and W.B. Joyner (1997). Site Amplifications for Generic Rock Sites, *Bull. Seismol. Soc. Am.* **87**, 327-341.

CEN (2003). Eurocode 8: Design of structures for earthquake resistance. Part 1: General rules, seismic actions and rules for buildings, (EN 1998-1: 2004). Brussels, Belgium.

Cotton F., F. Scherbaum, J.J. Bommer, H. Bungum (2006). Criteria for selecting and adjusting ground-motion models for specific target regions: Application to Central Europe and rock sites, *J. Seismol.* **10**, 137-156.

Douglas, J., Bungum, H. and Scherbaum, F. (2006). Ground motion prediction equations for southern Spain and southern Norway obtained using the composite model perspective, *J. Earthq. Eng.* **10**, 33–72.

Douglas, J., P. Gehl, L. F. Bonilla and C. Gélis (2010). A κ Model for Mainland France, *Pure Appl. Geophys.* **167**, 1303-1315.

Drouet S., F. Cotton, P. Gueguen (2010). Vs_{30}, κ, regional attenuation and Mw from accelerograms: application to magnitude 3–5 French earthquakes, *Geophys. J. Int.* **182**, 880-898.

Drouet S, S. Chevrot, F. Cotton, and A. Souriau (2008a). Simultaneous inversion of source spectra, attenuation parameters and site responses. Application to the data of the French Accelerometric Network, *Bull. Seism. Soc. Am.* **98**, 198-219.

Drouet S., N. Theodulidis and A. Savvaidis (2008b). Site effects from parameterised generalised inversions. ESC 31st General Assembly, Hersonissos, Crete, Greece, 8-12 Sept.

Edwards B., D. Fah and D. Giardini (2011). Attenuation of seismic shear wave energy in Switzerland. *Geophys. J. Int.* **185**, 967–984.

Goldstein, P., D. Dodge, M. Firpo, and L. Minner (2003). SAC2000: Signal processing and analysis tools for seismologists and engineers, The IASPEI International Handbook of Earthquake and Engineering Seismology, W.H.K. Lee, H. Kanamori, P.C. Jennings, C. Kisslinger (Editors), Academic Press, London.

Hanks, T. C. (1982). fmax, *Bull. Seismol. Soc. Am.* **72**, 1867-1879.

Hatzidimitriou, P., C. Papazachos, A. Kiratzi, and N. Theodulidis (1993). Estimation of attenuation structure and local earthquake magnitude based on accleration records in Greece, *Tectonophysics* **217**, 243–253.

Hatzidimitriou, P. (1995). S-wave attenuation in the crust in Northern Greece, *Bull. Seism. Soc. Am.* **85**, 1381-1387.

Hough, S.E., J.G. Anderson, J. Brune, F. Vernon, J. Berger, J. Fletcher, L. Haar, T. Hanks, and L. Baker (1988). Attenuation near Anza, California, *Bull. Seism. Soc. Am.* **78**, 672-691.

Konno, K. and Ohmachi, T. (1998). Ground-motion characteristics estimated from spectral ratio between horizontal and vertical components of microtremor, *Bull. Seismol. Soc. Am.* **88**, 228-241.

Ktenidou O.J., C. Gelis, L.F. Bonilla (2012). A study on the variability of kappa in a borehole. Implications on the computation method used. *Bull. Seismol. Soc. Am.* (submitted).

Luzi L., R. Puglia, F. Pacor, M.R. Gallipoli, D. Bindi, M. Mucciarelli (2011). Proposal for a soil classification based on parameters alternative or complementary to Vs,30, *Bull. Earthq. Eng.* **9**, 1877-1898.

Manakou M.V., D.G. Raptakis, F.J. Chavez-Garcıa, P.I. Apostolidis, K.D. Pitilakis (2010). 3D soil structure of the Mygdonian basin for site response analysis, *Soil Dyn. Earthq. Eng.* **30**, 1198–1211.

Mena, B., P. M. Mai, K. B. Olsen, M. D. Purvance, and J.N. Brune (2010). Hybrid broadband ground-motion simulation using scattering Greens functions: Application to large-magnitude events, *Bull. Seismol. Soc. Am.* **100**, 2143–2162.

Parolai S. and D Bindi (2004). Influence of Soil-Layer Properties on k Evaluation, Seism. Soc. Am. **94**, 349-356.

Pitilakis, K., Anastasiadis, A., & Riga, E. (2011a). New soil classification system and spectral amplification factors for EC8, in Proceedings of ISSMGE - ERTC 12 Workshop on Evaluation of Geotechnical Aspects of EC8, XV European Conference on Soil Mechanics and Geotechnical Engineering, M. Maugeri (Editor), Athens, 11 September 2011, Part 1, Ch. 6.

Raptakis D., F.J. Chavez-Garcıa, K. Makra, K. Pitilakis (2000). Site effects at Euroseistest—I. Determination of the valley structure and confrontation of observations with 1D analysis. *Soil Dyn. Earthq. Eng.* **19**, 1-22.

Silva, W., Darragh, R., Gregor, N., Martin, G., Abrahamson, N. and Kircher, C. (1998). Reassessment of site coefficients and near-fault factors for building code provisions, Technical Report Program Element II: 98-HQGR-1010, Pacific Engineering and Analysis, El Cerrito, USA.

Toro, G. R., N. A. Abrahamson, and J. F. Schneider (1997). Model of strong ground motions from earthquakes in central and eastern North America: Best estimates and uncertainties, *Seismol. Res. Lett.* **68**, 41–57.

Tsai, C.-C. P., and K.-C. Chen (2000). A model for the high-cut process of strong motion accelerations in terms of distance, magnitude, and site condition: an example from the SMART 1 array, Lotung, Taiwan, *Bull. Seism. Soc. Am.* **90**, 1535-1542.

Van Houtte C., Drouet C. and F. Cotton (2011). Analysis of the origins of κ (Kappa) to compute hard rock to rock adjustment factors for GMPEs, *Bull. Seism. Soc. Am.* **101**, 2926-2941.

Wessel, P., and W. H. F. Smith (1998). New, improved version of the Generic Mapping Tools Released, *EOS Trans. AGU* **79**, 579.